Magnesium Technology 2012
Edited by: Suveen N. Mathaudhu, Wim H. Sillekens, Neale R. Neelameggham, and Norbert Hort
TMS (The Minerals, Metals & Materials Society), 2012

EFFECT OF STRAIN RATE ON DYNAMIC RECRYSTALLIZATION IN A MAGNESIUM ALLOY UNDER COMPRESSION AT HIGH TEMPERATURE

Q. Ma[1], B. Li[1], A.L. Oppedal[1], W. Whittington[1], S.J. Horstemeyer[1], E.B. Marin[1], H. El. Kadiri[1,2], P.T. Wang[1], M.F. Horstemeyer[1,2]
[1]. Center for Advanced Vehicular Systems, Mississippi State University, Starkville, MS 39759, USA
[2]. Department of Mechanical Engineering, Mississippi State University, Starkville, MS 39762, USA

Keywords: Magnesium; Texture; Twinning; Non-basal slip; Dynamic Recrystallization.

Abstract

Interrupted uniaxial compression tests were performed on an extruded Mg-Al-Mn magnesium alloy (AM30) at 450°C and various strain rates of 0.001 s^{-1}, 0.1 s^{-1}, 0.5 s^{-1} and 0.8 s^{-1}. Texture and microstructure evolution were examined using electron back scattered diffraction (EBSD) and X-ray diffraction (XRD) techniques. Twinning was found to be ubiquitous at high temperature but provided that a highly enough strain rate was applied. The results show that the deformation microstructure evolves with strong dependence on the strain rate as twinning triggers and non-basal slips become harder. Schmid's factor and slip traces analyses elucidated the driving forces controlling dynamic recrystallization mechanisms and emphasized on the role played by extension twinning and non-basal slips.

Introduction

Dynamic recrystallization (DRX) is of particular importance for Mg and its alloys because DRX alters the microstructure of Mg during thermomechanical processing at temperatures normally above Mg's recovery and recrystallization point. DRX in Mg has been investigated in substantial experimental studies where it was correlated with deformation modes which are temperature dependent [1-4]. Sitdikov and Kaibyshev [1,2] investigated DRX of Mg in compression over a wide range of temperatures (20-500°C) at a constant strain rate 3×10^{-3} s^{-1}. They found that between 20°C and 350°C, twinning plays an important role in which crystallites result from mutual intersection of primary twins and/or secondary twins serve as nuclei. Between 250°C and 500°C, continuous dynamic recrystallization (CDRX) dominates via nucleation by subgrain rotation. At 450°C, grain boundary bulging also occurs via parent grain boundary migration in coarse grains. In addition, the pre-existing annealing twin boundaries can also evolve to large angle boundaries and then migrate by bulging mechanism [1,2]. Ion et al. [3] studied the DRX of Mg-0.8Al% alloy under compression between 150°C and 370°C at a strain rate 10^{-5} s^{-1}. They assumed a "rotation" mechanism of DRX, which explained well the phenomenon of "necklace" grains in Mg. Galiyev et al. [4] suggested other DRX mechanisms based on experimental results of Mg compression between 150°C and 450°C. At low temperatures (below 200°C), DRX is associated with operation of twinning, basal slip and <c+a> slip; between 200°C and 250°C, CDRX dominates via cross-slip; at high temperatures (between 300°C and 450°C), both bulging and subgrain growth play a crucial role in DRX. These mechanisms were revealed in deformation at a constant strain rate in their study.

It is well known that deformation mechanisms in crystalline metals strongly depend upon strain rate [5]. Hence, strain rate should presumably have a vital influence on DRX because activation of twinning, for example, strongly depends upon strain rate. On the other hand, non-basal slip modes, i.e. prismatic and pyramidal slip, become more active at high temperatures [6,7]. Thus, change in strain rate can lead to mechanistic complication in DRX in Mg alloys. In thermomechanical processing of Mg alloys, the strain rate can significantly vary depending upon the geometry of the work piece and tooling fixture and the speed (e.g. ram speed in extrusion). Even in the same work piece that is undergoing thermomechanical processing, the strain rate can be inhomogeneous and different from one location to another. Therefore, it is necessary to investigate how change in strain rate influences DRX. The objective of this work is to study DRX mechanisms in an extruded commercial AM30 Mg alloy under uniaxial compression at 450°C at various strain rates: 0.001 s^{-1}, 0.1 s^{-1}, 0.5 s^{-1} and 0.8 s^{-1}, based on electron back scattered diffraction (EBSD) analysis.

Experimental

An extruded commercial AM30 magnesium alloy (mass: Al 2.54%, Mn 0.40%, Mg balance) was selected as the experimental material. Right cylindrical samples 10 mm in diameter were cut by electrical-discharge machining (EDM), with the axial direction parallel to the extrusion direction (ED). Before uniaxial compression, the sample to be tested was heated to 450°C in the furnace that houses the sample stage of the INSTRON 5869 machine, and the temperature was maintained constant. Then the samples were compressed inside the furnace at different strain rates: 0.001 s^{-1}, 0.1 s^{-1}, 0.5 s^{-1} and 0.8 s^{-1}. The compression test of each sample was interrupted during plastic flow, and the sample was immediately quenched in water to preserve the microstructure. Then the micro-textures of the samples were examined using EBSD.

The true stress-strain curves of the AM30 at 450°C at different strain rates are presented in Figure 1. The yield stress and the flow stress increase with increasing strain rate. At strain rates 0.001 s^{-1} and 0.1 s^{-1}, the strain hardening is minimal. The stress-strain curve of 0.5 s^{-1} shows barely recognizable hardening, followed by a slight softening. When the strain rate increases to 0.8 s^{-1}, the stress-strain behavior exhibits an apparent sigmoidal shape of appreciable hardening, with a peak stress followed by a pronounced softening. The stress-strain curves at 0.001 s^{-1} and 0.1 s^{-1} present a parabolic shape in which dislocation slip dominates the plastic flow.

The microstructure and microtexture evolution during compression in ED at various strain rates is shown in Figure 2. The inverse pole figure (IPF) maps are shown as well. Figure 2a shows the initial micro-texture and microstructure of the untested sample. We can see that the initial microstructure consists of a mixture of coarse grains and dynamically recrystallized fine grains created during extrusion. In the pole figure, the basal planes are roughly parallel to the ED (or $\langle 10\bar{1}0\rangle \parallel$ ED), which is typical of extruded Mg alloys. Figure 2b shows homogenous, equiaxed

grains at 0.001 s^{-1} and $\varepsilon = -0.15$, indicating a full recrystallization, i.e., nucleation and ripening in comparison to the initial state (Figure 2a). Figure 2c presents the microstructure at 0.1 s^{-1} and $\varepsilon = -0.15$ in which lenticular twins in red start emerging. Twinning is confirmed by the ~90° rotation in {0001} pole figure which is caused by the presence of $\{10\bar{1}2\}\langle 10\bar{1}\bar{1}\rangle$ twins. When the strain rate increases to 0.5 s^{-1}, as shown in Figure 2d, profuse, large $\{10\bar{1}2\}\langle 10\bar{1}\bar{1}\rangle$ twins can be seen in a coarse, non-recrystallized grain, in addition to the small twins in the fine grains. A strong basal texture can be observed in the pole figure. In the mean time, dynamically recrystallized, "necklace" grains nucleate and grow, surrounding the parent grains, then some invading into the matrix along twin boundaries. Figures 2e and 2f show the microstructure at 0.8 s^{-1}, $\varepsilon = -0.04$ and -0.15, respectively. The $\{10\bar{1}2\}\langle 10\bar{1}\bar{1}\rangle$ twinning dominates the deformation and leads to an enhanced basal texture. At $\varepsilon = -0.04$, high density twins can be observed. Meanwhile, fine "necklace" grains surrounding parent grains nucleate and grow. At $\varepsilon = -0.15$, the twins grow significantly, coalesce and consume most of the grains. The dynamically recrystallized necklace grains are sandwiched between the impinged twins. New grains may also nucleate inside the twins and grow, eventually segmenting the large twins into irregular islands. No $\{10\bar{1}1\}\langle 10\bar{1}2\rangle$ contraction twin or $\{10\bar{1}1\}-\{10\bar{1}2\}$ double twins were found in this study.

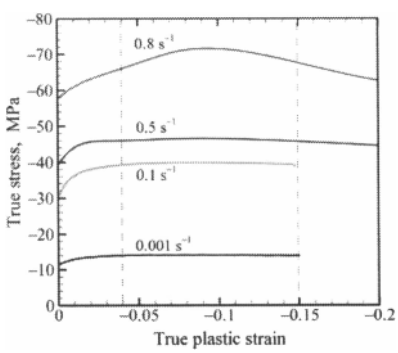

Figure 1: The uniaxial compression true stress true strain curves of AM30 at 450°C and strain rates: 0.001 s^{-1}, 0.1 s^{-1}, 0.5 s^{-1} and 0.8 s^{-1}.

Macrotexture of the AM30 samples was also measured on a Rigaku SmartLab X-Ray Diffractometer (XRD). The six incompleted pole figures, $\{10\bar{1}0\}$, {0002}, $\{10\bar{1}1\}$, $\{10\bar{1}2\}$, $\{11\bar{2}0\}$ and $\{10\bar{1}3\}$ were measured by X-ray, and background and defocusing effect was eliminated. The Orientation Distribution Function (ODF) was calculated based on the measured pole figures. The recalculated pole figures were calculated based on the ODF. The macrotexture of AM30 samples are presented in Figure 3. The macrotexture measured by XRD definitely prove the presence of $\{10\bar{1}2\}$ twinning (Figures 3). Twinning induced a strong basal texture at ε=-0.04 and at higher strain rates of 0.5 s^{-1} and 0.8 s^{-1} (Figure 3b,3c)

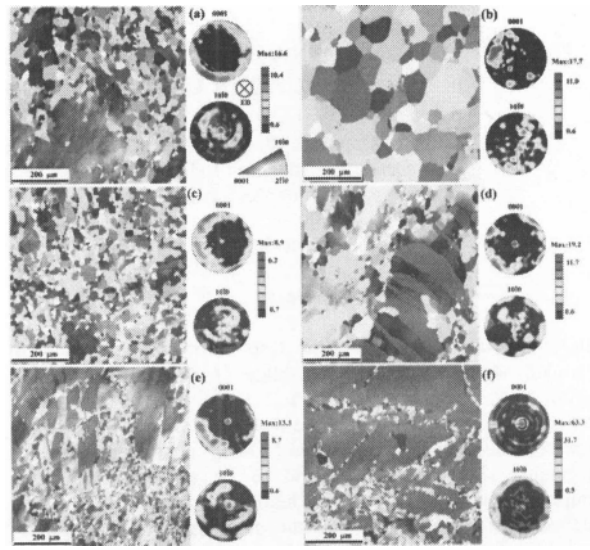

Figure 2. EBSD inverse pole figure map and micro-texture of AM30 under uniaxial compression at 450°C at (a) initial status; (b) 0.001 s^{-1}, ε=-0.15, grains become coarse and equiaxed; (c) 0.1 s^{-1}, ε=-0.15, visible thin $\{10\bar{1}2\}\langle 10\bar{1}\bar{1}\rangle$ twins appear; (d) 0.5 s^{-1}, ε=-0.04, thick twins locate in parent grain and "necklace" grains appear and some of them grow along twin interfaces; (e) 0.8 s^{-1}, ε=-0.04, twinning propagates in both parent grains and recrystallized grains, and (f) 0.8 s^{-1}, ε=-0.15, twinning sweeps almost whole parent grains and results in a very strong basal texture, and DRX evolves inside twinned parent grain. The pole figures are calculated based on the corresponding EBSD maps. The inverse pole figure represents the compression direction, namely the extrusion direction (ED).

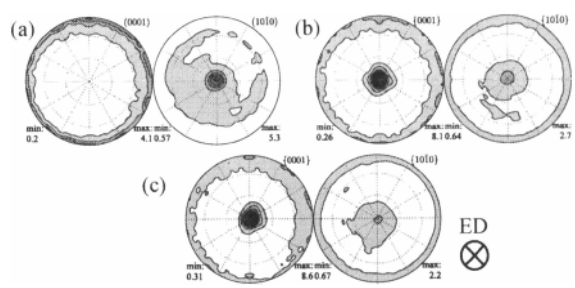

Figure 3. XRD macrotexture of AM30 uniaxial compression along ED at 450°C and at (a) initial state; (b) $\dot{\varepsilon}$=0.5 s^{-1}, ε=-0.04, a strong basal texture appears which induced by $\{10\bar{1}2\}$ twinning; (c) $\dot{\varepsilon}$=0.8 s^{-1}, ε=-0.04, a strong basal texture resulted by $\{10\bar{1}2\}$ twinning. Intensity levels: 1,2,3,4,5,6,7,8.

Discussion

At the quasi-static strain rate 0.001 s^{-1}, the stress-strain curve of 0.001 s^{-1} (Figure 1) shows no hardening. This is because at this slow strain rate, the overall dislocation density is balanced between dislocation accumulation by proceeding deformation and dislocation annihilation by recovery, DRX and subsequent grain growth. Galiyev et al. [4] suggested that DRX is accomplished by subgrain rotation or new grain nucleation and growth inside the parent grains. The main active slip modes should be prismatic and pyramidal slip because (1) the critical resolved shear stress (CRSS) of the prismatic and pyramidal slip is close to that of basal slip at 450°C and low strain rate [6]; (2) the Schmid factor (SF) of prismatic and pyramidal slip is greater than 0.4 near

$\langle 10\bar{1}0\rangle$, in contrast to nearly zero for basal slip (see calculations in Figures 4c to 4e). The initial texture of AM30 (Figures 3a, 4a), measured by X-ray diffraction (XRD), definitely favors $\{10\bar{1}2\}\langle 10\bar{1}\bar{1}\rangle$ twinning because this twinning mode has a maximum SF of 0.5 around $\langle 10\bar{1}0\rangle$ (Figure 4b). However, twinning is suppressed by slip because the flow stress does not reach the CRSS of twinning at strain rate 0.001 s^{-1}.

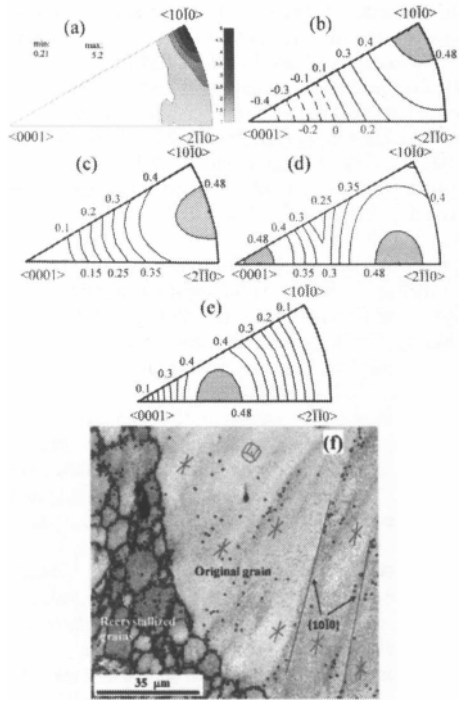

Figure 4. (a) Inverse pole figure of the extrusion direction (ED) for initial AM30 at 450°C by XRD. The Schmid factor distribution in the inverse pole figure compression by the deformation mode of (b) $\{10\bar{1}2\}\langle 10\bar{1}\bar{1}\rangle$ twinning; (c) prismatic $\langle a\rangle$: $\{10\bar{1}0\}\langle 11\bar{2}0\rangle$ slip; (d) second order pyramidal $\langle c+a\rangle$: $\{11\bar{2}2\}\langle 11\bar{2}\bar{3}\rangle$ slip; and (e) basal $\langle a\rangle$: $\{0001\}\langle 11\bar{2}0\rangle$ slip. (f) Prismatic $\langle a\rangle$: $\{10\bar{1}0\}\langle 11\bar{2}0\rangle$ slip traces in EBSD image quality map at 0.8 s^{-1}, ε=-0.04. The slip lines prove abundant prismatic $\langle a\rangle$ slips in the parent grain. The red lines and stars in Figure 3f are the $\{10\bar{1}0\}$ plane traces, the dark lines represent large angle grain boundaries (LAGB) >15°.

Barnett et al. [8,9] studied flow stress of AZ31 Mg alloy deformation at 300°C and 350°C at various strain rates. With increasing strain rate, the plateau of the flow curve shifts to a marked sigmoidal flow curve, which is attributed to the possible twinning. Ishikawa et al. [10] and Myshlyaev et al. [11] observed twins in Mg at 400°C and 450°C first at high strain rate (10^3 s^{-1}) by optical microscopy (OM), then at low strain rate of 0.01 s^{-1} by transmission electron microscopy (TEM). In our previous study [12], profuse $\{10\bar{1}2\}\langle 10\bar{1}\bar{1}\rangle$ twinning was observed in an AZ61 Mg alloy extruded at 450°C, which played an important role in DRX. There are others' results that show absence of deformation twinning in Mg at temperatures greater than ~400°C and strain rates less than 0.01 s^{-1} [1-4,13]. In fact, twinning is athermal in hcp metals [7]. The CRSS of twinning should be insensitive to temperature, while twin nucleation and growth propagation mainly depend upon local stress state that is rate dependent.

When strain rate increases to 0.1 s^{-1}, new grains mainly nucleate at the interior of the parent grains (Figure 2c). Similar to the quasi-static case (0.001 s^{-1}), pyramidal and prismatic slip are activated mainly in the parent grains. The grain structure is much finer compared with strain rate 0.001 s^{-1}, owing to growth kinetics (Figure 2b, 2c). Sporadic $\{10\bar{1}2\}\langle 10\bar{1}\bar{1}\rangle$ twins can be seen inside some of the parent grains (Figure 2c), indicating the flow stress may be just above the CRSS of twinning.

At relatively high strain rates, 0.5 s^{-1} and 0.8 s^{-1}, prismatic slip should still be active in the parent grains because it has high SF values around $\langle 10\bar{1}0\rangle$ (Figure 4c). Figure 4f shows slip trace analysis by EBSD at strain rate 0.8 s^{-1} and strain level $\varepsilon = -0.04$. It is clear that prismatic slip is indeed the main active slip mode in the parent grain. The stress concentration near parent grain boundaries may trigger the pyramidal slip to accommodate strain because the prismatic slip has only two independent systems. The pyramidal slip alone can provide five independent slip systems that fulfill the von Mises criteria to accommodate polycrystalline plastic strain. Thus, parent grain boundaries become favorable nucleation sites for DRX due to the activation of the non-basal slip modes.

The formation of the "necklace" grains was attributed to the "rotation recrystallization" induced by the pyramidal slip in Mg, as suggested by Ion et al. [3]. Some grains grow along twin boundaries due to the possible pyramidal slip at twin/matrix interfaces. Yoo [14] assumed that the twin boundaries, in addition to grain boundaries, are another important source of pyramidal slip. High density pyramidal dislocations at twin boundaries were observed in TEM by Agnew et al. [15] and Morozumi et al. [16]. Accordingly, the dynamically recrystallized grains grow at the expense of the twins, giving rise to the softening by DRX as seen in the stress-strain responses at strain rates 0.5 s^{-1} and 0.8 s^{-1}. In Figure 2f, some new grains are nucleated inside the largely twinned grains. This can be understood from the fact that the orientation of the twins favors pyramidal slip because the SF is high (Figure 4d). As such, pyramidal slip is activated in the twins (Figure 2f) and facilitates DRX inside the twins. Note that some grains are nucleated along the prismatic slip traces (Figure 4f), indicating that the prismatic slip may also be favorable for nucleation due to the high plastic energy and short-circuit diffusion paths in the dislocation pipe-lines.

Moreover, twinning almost saturates at the strain level $\varepsilon = -0.15$ at strain rate 0.8 s^{-1} (Figure 2f). Accordingly, a distinct softening occurs following the peak flow stress (Figure 1). It is the competition between hardening by twinning versus softening by DRX that results in an apparent peak stress followed by a softening, as shown in the stress-strain curve at strain rate 0.8 s^{-1}.

Finally, according to observation and analysis, the effect of strain rate on DRX of the AM30 compressed at 450°C is schematized in Figure 5. At low strain rate, nucleation and grain growth in the parent grain interior dominates the DRX. Due to the low strain rate, the recrystallized grain size ripens, as shown in Figure 4a. At intermediate strain rate, DRX proceeds primarily at the grain boundaries, most likely via the activation of non-basal slip; meanwhile, twinning propagates inside the parent grains. Some new grains may grow along twin boundaries (Figure 5b). At high strain rates, twinning dominates the plastic deformation, with fine grains nucleate along parent grain boundaries; subsequently DRX evolves quickly in the twinned parent grain (Figure 5c). As our experiments clearly demonstrate, the size of the dynamically recrystallized grains, while at the same strain level, decreases as the strain rate increases.

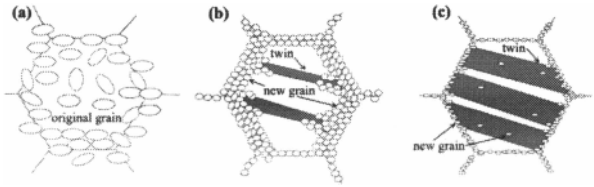

Figure 5. Schematic illustration of dynamic recrystallization in the AM30 alloy compression at 450°C and various strain rates: (a) Low strain rate, (b) intermediate strain rate, and (c) high strain rate.

Conclusions

In summary, we investigated the effect of strain rate on DRX at 450°C in an extruded AM30 alloy. Compression tests were performed at strain rates 0.001 s^{-1}, 0.1 s^{-1}, 0.5 s^{-1} and 0.8 s^{-1}. Texture evolutions in quenched samples were examined by EBSD and XRD. The stress-strain responses strongly depended on the strain rate. At quasi-static strain rate 0.001 s^{-1}, no strain hardening was observed and equiaxed, ripened grains were formed. DRX is accomplished by subgrain rotation or new grain nucleation and growth inside the parent grains [4]. At relatively low strain rate, 0.1 s^{-1}, a finer grain structure was obtained and sporadic deformation twins were present; again, no strain hardening was observed. The mechanism of DRX is nucleation and growth of new grains inside the interior of the parent grains. At intermediate strain rate, 0.5 s^{-1}, strain hardening was barely recognizable, followed by a slight softening; an increase in twin volume fraction was observed. At high strain rate, 0.8 s^{-1}, the stress-strain response presents a sigmoidal behavior, with a peak flow stress followed by a distinct softening. At high strain rates, the dominant mechanism of DRX is the activation of non-basal slip modes at the grain boundaries, and fine, necklace grains are nucleated surrounding the parent grains. In the mean time, the growth of the dynamically recrystallized grains along the twin boundaries consumes the twins, leading to irregular morphology of the twins as the strain is increased.

Acknowledgements

The authors are grateful to the financial support from the Department of Energy, Contract No. DE-FC-26-06NT42755, and the Center for Advanced Vehicular Systems (CAVS) at Mississippi State University.

References

1. O. Sitdikov and R. Kaibyshev, "Dynamic recrystallization in pure magnesium", *Materials Transactions*, 42 (2001), 1928-1937.
2. R.O. Kaibyshev and O. Sh. Sitdikov, "On the role of twinning in dynamic recrystallization", *The Physics of Metals and Metallography*, 89 (2000), 70-77.
3. S.E. Ion, F.J. Humphreys and S.H. White, "Dynamic recrystallization and the development of microstructure during the high temperature deformation of magnesium", *Acta Metallurgica*, 30 (1982), 1909-1919.
4. A. Galiyev, R. Kaibyshev and G. Gottstein, "Correlation of plastic deformation and dynamic recrystallization in magnesium alloy ZK60", *Acta Materialia*, 49 (2001), 1199-1207.
5. M.A. Meyers, O. Vöhringer and V.A. Lubarda, "The onset of twinning in metals: a constitutive description", *Acta Materialia*, 49 (2001), 4025-4039.
6. A. Chapuis and J.H. Driver, "Temperature dependency of slip and twinning in plane strain compressed magnesium single crystals", *Acta Materialia*, 59 (2011), 1986-1994.
7. A. Jain and S.R. Agnew, "Modeling the temperature dependent effect of twinning on the behavior of magnesium alloy AZ31B sheet", *Materials Science and Engineering*, A 462 (2007), 29-36.
8. M.R. Barnett, "Influence of deformation conditions and texture on the high temperature flow stress of magnesium AZ31", *Journal of Light Metals*, 1 (2001), 167-177.
9. A.G. Beer and M.R. Barnett, "Microstructural development during hot working of Mg-3Al-1Zn", *Metallurgical and Materials Transactions A*, 38A (2007), 1856-1867.
10. K. Ishikawa, H. Watanabe and T. Mukai, "High strain rate deformation behavior of an AZ91 magnesium alloy at elevated temperatures", *Materials Letters*, 59 (2005), 1511-1515.
11. M.M. Myshlyaev, et al., "Twinning, dynamic recovery and recrystallization in hot worked Mg-Al-Zn alloy", *Materials Science and Engineering*, A 337 (2002), 121-133.
12. Q. Ma, et al., "Twinning-induced dynamic recrystallization in a magnesium alloy extruded at 450 °C", *Scripta Materialia*, 65 (2011), 823-826.
13. T. Al Samman and G. Gottstein, "Dynamic recrystallization during high temperature deformation of magnesium", *Materials Science and Engineering*, A490 (2008), 411-420.
14. M.H. Yoo, "Slip, twinning, and fracture in hexagonal close-packed metals", *Metallurgical Transactions*, A12 (1981), 409-418.
15. S.R. Agnew, J.A. Horto and M.H. Yoo, "Transmission electron microscopy investigation of <c+a> dislocations in Mg and α-solid solution Mg-Li alloys", *Metallurgical and Materials Transactions*, 33A (2002), 851-858.
16. S. Morozumi, M. Kikuchi and H. Yoshinaga, "Electron microscope observation in and around {1-102} twins in magnesium", *Transactions of the Japan Institute of Metals*, 17 (1976), 158-164.